Available online at www.sciencedirect.com
SCIENCE DIRECT®
ELSEVIER
Nuclear Instruments and Methods in Physics Research B 233 (2005) 307–311
NIM B Beam Interactions with Materials & Atoms
www.elsevier.com/locate/nimb

Ionization of helium in positron impact

K. Tőkési [a,b], I.F. Barna [b,*], J. Burgdörfer [b]

[a] *Institute of Nuclear Research of the Hungarian Academy of Science (ATOMKI), P.O. Box 51, H-4001 Debrecen, Hungary, EU*
[b] *Institute for Theoretical Physics, Vienna University of Technology, A-1040 Vienna, Austria, EU*

Available online 25 April 2005

Abstract

We present single-ionization cross sections of helium for positron impact within the framework of classical trajectory Monte Carlo (CTMC) method and compare with Coulomb distorted-wave models and experimental data. The incident positron energy was varied between the ionization threshold and 500 eV. Our results are in agreement with the experimental data. We also present ionization cross sections where the He^{+} ion remains either in the 1s ground state or is simultaneously excited into the 2s or 2p state.

PACS: 34.85.+x

Keywords: Positron; Ionization; CTMC; Distorted-wave models

1. Introduction

Ionization of helium by positron impact has been extensively studied both theoretically and experimentally [1–5] during the last decades. The first quantum-mechanical calculation of the ionization cross section for positron impact of helium was carried out with the first-order Born approximation by Basu et al. [6]. The first classical trajectory Monte Carlo (CTMC) calculation was carried out by Schultz and Olson [7]. The time-dependent coupled-channel method was implemented with hyperbolic positron trajectories in the energy range of 6–1000 eV by Chen and Msezane [8]. A more elaborate coupled-channel method was presented in [9] including positronium formation. A distorted-wave method with close-coupled target states was applied to calculate the total ionization cross sections for noble gases in positron impact up to about 1 keV [10].

In this work we present single-ionization cross sections of helium following positron impact. Our equivalent electron and non-equivalent electron CTMC calculations are compared with the Coulomb distorted-wave Born approximation (CDWBA) and with the experimental data. We

* Corresponding author.
E-mail address: barna@concord.itp.tuvien.ac.at (I.F. Barna).

0168-583X/$ - see front matter © 2005 Published by Elsevier B.V.
doi:10.1016/j.nimb.2005.03.127

also present partial ionization cross sections where the He^+ ion remains either in the 1s ground state or excited into the 2s or 2p states. Atomic units are used throughout the paper unless otherwise indicated.

2. Theory

2.1. Classical trajectory Monte Carlo approximations

In both versions of the present CTMC approach, Newton's classical non-relativistic equations of motions for a three- or four-body system are solved numerically for a statistically large number of trajectories for given initial conditions. The equations of motion were integrated using a standard Runge–Kutta method.

2.2. Non-equivalent electron CTMC model (NEE-CTMC)

The four structureless particles are characterized by their masses and charges. The forces acting among the four bodies are taken to be Coulombic. The interaction between the two active electrons of the helium atom is neglected during the collision. The impact parameter of the projectile as well as the positions and the velocities of the electrons moving in the field of the target nucleus are randomly chosen. The binding energies of the electrons in the He atom are set to 2 a.u. and 0.903 a.u., respectively [11,12]. The various final states are identified at large distances from the collision center. For the case of the ionization with simultaneous excitation, the classical n-level for the remaining bound electron can be assigned according to

$$n_c = q\sqrt{\mu/2U}; \tag{1}$$

where q is the charge of the target nucleus, U is the binding energy of the electron and μ is the reduced mass of the electron and its ionic nucleus. Similarly, the classical orbital angular momentum of the bound electron can be defined by

$$l_c = [(x\dot{y} - y\dot{x})^2 + (x\dot{z} - z\dot{x})^2 + (y\dot{z} - z\dot{y})^2]^{1/2}, \tag{2}$$

where x, y, z are the Cartesian coordinates of the electron relative to the target nucleus. According to Becker and MacKellar [13], the classical values of n_c can be "quantized" in terms of a quantum level n satisfying the following relation:

$$[(n-1)(n-1/2)n]^{1/3} \leqslant n_c \leqslant [n(n+1/2)(n+1)]^{1/3}. \tag{3}$$

The classical orbital angular momentum can also be mapped onto an angular momentum quantum number l satisfying the following relation [13]:

$$l \leqslant l_c n/n_c \leqslant l+1. \tag{4}$$

The total cross section for a specific event i is calculated from

$$\sigma_i = \frac{2\pi b_{\max} \sum b_i}{N}. \tag{5}$$

The statistical uncertainty for a cross section is given by:

$$\Delta\sigma_i = \sigma_i \left(\frac{N - N_i}{N N_i}\right)^{1/2}. \tag{6}$$

In Eqs. (5) and (6) N is the total number of the trajectories calculated for the impact parameters less than $b_{\max}$, N_i is the number of trajectories that satisfy the criteria for the process under consideration, b_i is the actual impact parameter for the event i specified by a set of collision product criteria.

2.3. Equivalent electron CTMC model (EE-CTMC)

The three particles in this model are the projectile, one atomic active electron (e^-) and the remaining helium ion (He^+). The interaction between the active target electron and the projectile is Coulombic. For the description of the interaction between the projectile and the helium core and between the active electron and the helium core a model potential is used which is based on Hartree–Fock calculations [14]:

$$V(r) = [(Z-1)\Omega(r) + 1]/r \tag{7}$$

where Z is the nuclear charge and

$$\Omega(r) = [Hd(e^{r/d} - 1) + 1]^{-1}. \tag{8}$$

Using energy minimization, Garvey et al. [15] obtained the following parameters for He: $H = 1.77$ a.u. and $d = 0.381$ a.u. The initial conditions of an individual collision are chosen at sufficiently large internuclear separation from the collision center, where the interactions among the particles are negligible. These initial conditions are selected as described by Reinhold and Falcon [16] for non-Coulombic systems. A microcanonical ensemble characterizes the initial state of the target. The initial conditions were taken from this ensemble, which is constrained to an initial binding energy of He(1s), 0.903 a.u. A three body, three-dimensional CTMC calculation is performed as described by Olson and Salop [17]. From the trajectory calculations we obtain the one-electron ionization probabilities as a function of the impact parameter b as

$$P_i(b) = \frac{N_i(b)}{N}. \tag{9}$$

The single-ionization cross section of He can be calculated as

$$\sigma_i^+ = 2\pi \int_0^\infty b2P_i(b)\,\mathrm{d}b. \tag{10}$$

2.4. Coulomb distorted-wave model

Our Coulomb distorted-wave model has been introduced in detail in our previous work [18] and here we give only a brief summary.

The model is defined by the Hamiltonian,

$$H = -\frac{1}{2}\nabla_\mathrm{p}^2 + H_\mathrm{He} + V_\mathrm{p\text{-}He}. \tag{11}$$

The first term stands for the kinetic energy of the positron, H_He is the unperturbed helium Hamiltonian and $V_\mathrm{p\text{-}He}$ is the interaction operator between the positron and the target helium,

$$V_\mathrm{p\text{-}He} = \frac{2}{R} - \frac{1}{|\mathbf{R}-\mathbf{r}_1|} - \frac{1}{|\mathbf{R}-\mathbf{r}_2|}, \tag{12}$$

$\mathbf{r}_1$, $\mathbf{r}_2$ and $\mathbf{R}$ are the coordinates of electrons 1 and 2 and the projectile positron with respect to the center of mass, respectively. We neglect any polarization effects. Considering that the velocity of the positron is large compared to the bound atomic electrons we apply the following first Born approximation formula from Mott and Massey [19] for the differential ionization cross section:

$$\frac{\mathrm{d}\sigma^\mathrm{ion}}{\mathrm{d}\Omega} = \sum_n |f_n(\theta,\phi)|^2, \tag{13}$$

where

$$\begin{aligned} f_n(\theta,\phi) = {} & \frac{4\pi^2\mu^2 k_0}{k_n} \\ & \times \int\int\int \mathrm{d}\mathbf{r}_1\,\mathrm{d}\mathbf{r}_2\,\mathrm{d}\mathbf{R}\,\varphi_n^*(\mathbf{R})\Psi_n^*(\mathbf{r}_1,\mathbf{r}_2) \\ & \times [V_\mathrm{p\text{-}He} - 1/R] \\ & \times \varphi_0(\mathbf{R})\Psi_\mathrm{g}(\mathbf{r}_1,\mathbf{r}_2), \end{aligned} \tag{14}$$

k_0 is the wavenumber of the incoming positron described by a plane wave $\varphi_0(\mathbf{R})$ and k_n is the wave number for the outgoing positron approximated by a Coulomb wave $\varphi_n(\mathbf{R})$ with charge $Z = 1$ because we calculate single-ionization. As for the initial helium state, $\Psi_\mathrm{g}(\mathbf{r}_1,\mathbf{r}_2)$, we take the helium ground state wavefunction obtained by diagonalizing the unperturbed helium Hamiltonian in a configuration interaction (CI) basis of orthogonalized two-particle functions. For the single-particle wavefunctions we use an angular momentum representation with spherical harmonics Y_l^m, hydrogen-like radial Slater functions and radial regular Coulomb wave packets. The wave packets form a discrete representation of the continuum which can be incorporated into our finite basis set. We used 28 different Coulomb wave packets in our basis with $Z = 1$ and $Z = 2$ different effective charges up to 4.4 a.u. mean energy to equidistantly cover the helium spectrum up to 10 a.u. The diagonalization process gives us 465 helium basis states. The method of the Coulomb wave packets and the CI wavefunctions calculation is described in [20]. For the $L = 0$ configurations we have used angular correlated wavefunctions to get a ground state energy of -2.901 a.u. which is reasonably accurate compared to the "exact" value of -2.903 a.u. For the $L = 1,2$ states only sp or sd configurations were taken.

To calculate the total ionization cross section, σ^ion, we sum over those CI helium states $\Psi_n^*(\mathbf{r}_1,\mathbf{r}_2)$ whose energies lie in the helium continuum and integrate over the solid angle $\mathrm{d}\Omega$. The energies of these single-ionized final helium states $\Psi_n^*(\mathbf{r}_1, \mathbf{r}_2)$ automatically define the energy of the outgoing positron described by a Coulomb wave through energy conservation.

To identify ionization channels leaving He^+ in the ground state or simultaneously excited into the 2s or 2p Rydberg state, we use the complex scaling method [21]. All single-ionization Rydberg states lie on different straight lines in the complex energy plane. These lines end on the real energy axis. These end points are the corresponding energy values of the ionized helium atom e.g. $He^+(1s)$.

3. Results and discussion

Fig. 1 shows the single-ionization cross sections of He in collision with positrons. Our recent results based on EE-CTMC and NEE-CTMC model together with the distorted-wave Born model are compared with the experimental data [1–5] and with the distorted-wave model calculations of Campeanu et al. [22]. It is worth to mention that all the presented data include the single-ionization contributions only. The incident positron energy is varied from the ionization threshold up to 500 eV. Between the first ionization threshold (24.56 eV) and 80 eV all the theoretical results are in good agreement with the experimental data. Above this energy NEE-CTMC results are about 60 percent smaller than the experimental and other theoretical data. This can be attributed to the fact that in NEE-CTMC approximation we completely neglect the electron–electron interaction while in EE-CTMC calculation it is partially taken into account via the distance dependent model potential. Above 80 eV our distorted-wave model is about 5 percent larger than the calculations of Campeanu et al. [22].

In the following we show the state selective ionization cross sections where the He^+ ion remains either in the 1s ground state or is simultaneously excited to the 2s or 2p state:

$$e^+ + He(1s^2) \rightarrow He^+(1s) + e^+ + e^-. \quad (15)$$

$$e^+ + He(1s^2) \rightarrow He^+(2s) + e^+ + e^-. \quad (16)$$

$$e^+ + He(1s^2) \rightarrow He^+(2p) + e^+ + e^-. \quad (17)$$

Fig. 2 shows the partial single-ionization cross sections described by Eqs. (15)–(17). As

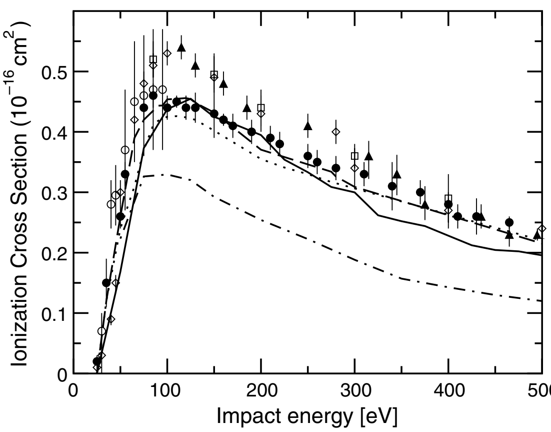

Fig. 1. Positron impact ionization cross sections of helium. Experimental data: (♦) Knudsen et al. [2]; (▲) Moxom et al. [5]; (●) Fromme et al. [1]; (○) Mori and Sueoka [3]; (□) Jacobsen et al. [4]. The solid line presents EE-CTMC and the dash-dotted line stands for NEE-CTMC results. The dashed curve shows our distorted-wave results and the dotted line presents the work of Campeanu et al. [22].

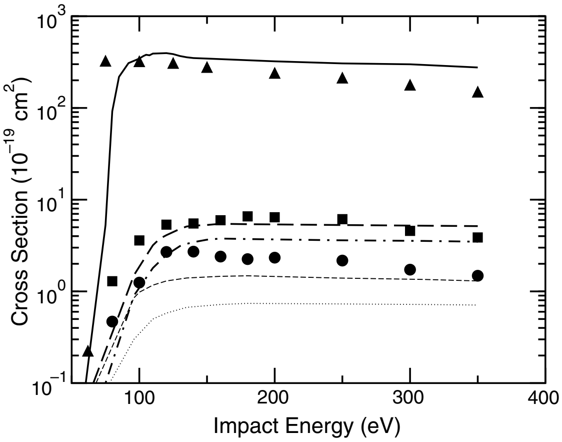

Fig. 2. Ionization cross sections of helium where the helium ion is in a well defined state expressed by Eqs. (15)–(17). The three full symbols stand for our NEE-CTMC results, ▲ for $He^+(1s)$, ■ for $He^+(2p)$ and (●) for $He^+(2s)$ reactions. The thick lines represent our distorted-wave results. The solid line is for $He^+(1s)$, dashed line for $He^+(2p)$ and the dash-dot-dashed line is for $He^+(2s)$. The dotted thin line shows the results of Moores [10] for $He^+(2s)$ and the thin dashed line stands for $He^+(2p)$.

we expected the dominant contribution to the ionization cross section arise from the channel where the bound target electron remains in the ground state after the collision. For the case of the ionization with simultaneous excitation (see Eqs. (16) and (17)) the cross sections are about two order of magnitude smaller. In Fig. 2 we also show the cross sections of ionization with simultaneous excitation obtained by the distorted-wave calculations of Moores [10]. The present cross sections based on the Coulomb distorted-wave model are about a factor of 4 larger than those of Moores. Due to the favorable dipole transition, ionization with excitation of the 2p state is larger than that with excitation of the 2s state. Similar effects were also observed for the excitation of helium by protons [23]. Unfortunately, no experimental data are available for these processes so far in the case of positron impact. We hope that our calculations together with the work of Moores stimulate experimentalists to measure the partial ionization cross sections for positron impact.

4. Summary

We have presented CTMC and Coulomb distorted-wave Born calculations and compared with experimental data for ionization of helium in positron impact. Both our CTMC and Coulomb distorted-wave model give reasonable agreement with the experimental data. Due to our Coulomb wave packet basis, our distorted-wave model represents the soft electron continuum of helium in a more detailed manner, and yields larger cross sections than the distorted-wave model of Campeanu et al. [22]. Partial cross sections for ionization and simultaneous excitation of the 2s and 2p states have also been calculated and compared to the distorted-wave calculations of Moores [10]. Our cross sections are 2–5 times larger than those of Moores.

Acknowledgements

The work was supported by the Hungarian Scientific Research Found: OTKA Nos. T046095, T046454, the Tét grant no. A-15/04, the grant "Bolyai" from the Hungarian Academy of Sciences, "Stiftung Aktion Österreich-Ungarn", No. 55öu1 and EU under contract no. HPRI-CT-2001-50036.

References

[1] D. Fromme, G. Kruse, W. Raith, G. Sinapius, Phys. Rev. Lett. 57 (1986) 3031.
[2] H. Knudsen, L. Brun-Nielsen, M. Charlton, M.R. Poulsen, J. Phys. B: At. Mol. Opt. Phys. 23 (1990) 3955.
[3] S. Mori, O. Sueoka, J. Phys. B: At. Mol. Opt. Phys. 27 (1994) 4349.
[4] M.F. Jacobsen, N.P. Frandsen, H. Knudsen, U. Mikkelson, D.M. Schrader, J. Phys. B: At. Mol. Opt. Phys. 28 (1995) 4691.
[5] J. Moxom, P. Ashley, G. Laricci a, Can. J. Phys. 74 (1996) 367.
[6] M. Basu, P.S. Mazumdar, A.S. Ghosh, J. Phys. B: At. Mol. Opt. Phys. 18 (1985) 369.
[7] D.R. Schultz, R.E. Olson, Phys. Rev. A 38 (1988) 1866.
[8] Z. Chen, A.Z. Msezane, Phys. Rev. A 49 (1993) 1752.
[9] C.P. Campbell, Mary T. McAlinden, Ann A. Keroghan, H.R.J. Walters, Nucl. Instr. and Meth. B 143 (1998) 41.
[10] L.D. Moores, Nucl. Instr. and Meth. B 179 (2001) 316.
[11] M.L. McKenzie, R.E. Olson, Phys. Rev. A 35 (1987) 2863.
[12] K. Tőkési, G. Hock, J. Phys. B: At. Mol. Opt. Phys. 30 (1997) L123.
[13] R.L. Becker, A.D. MacKellar, J. Phys. B: At. Mol. Opt. Phys. 17 (1987) 3923.
[14] A.E.S. Green, Adv. Quantum Chem. 7 (1973) 221.
[15] R.H. Garvey, C.H. Jackman, A.E.S. Green, Phys. Rev. A 12 (1975) 1144.
[16] C.O. Reinhold, C.A. Falcon, Phys. Rev. A 33 (1986) 3859.
[17] R.E. Olson, A. Salop, Phys. Rev. A 16 (1977) 531.
[18] I.F. Barna, Eur. Phys. J.D 30 (2004) 5.
[19] N.F. Mott, H.S.W. Massey, The Theory of Atomic Collision, third ed., Clarendon, Oxford, 1965.
[20] I.F. Barna, Doctoral thesis, University Giessen (2002); http://geb.uni-giessen.de/geb/volltexte/2003/1036.
[21] M. Moiseyev, Phys. Rep. 302 (1998) 211.
[22] R.I. Campeanu, R.P. McEachron, A.D. Stauffer, Nucl. Instr. and Meth. B 192 (2002) 146.
[23] D. Bodea, A. Orbán, D. Ristoiu, L. Nagy, J. Phys. B: At. Mol. Opt. Phys. 31 (1998) L745.